Geophys. J. R. astr. Soc. (1982) **68**, 487–497

Phase boundaries in finite amplitude mantle convection

Ulrich Christensen* *Institut für Geophysik und Meteorologie der Technischen, Universität Braunschweig, Mendelssohnstrasse 1a, D-3300 Braunschweig, West Germany*

Received 1981 June 10; in original form 1980 February 7

Summary. Phase boundaries are included in dynamical finite element models of mantle convection. They are represented by point chains which act as additional sources of buoyancy forces when distorted, and as additional source or sink of heat. The influence of the exothermic olivine-spinel transition is studied in both shallow and deep convection models. The flow is only slightly enhanced by the transition. The increase of temperature due to latent heat release is step-like in the deep model, in the case of shallow convection it is more diffuse. Other quantities like ocean-floor topography, gravity anomalies, and stress distribution are no more than moderately affected. In a further investigation the effect of spinel post-spinel transition, whether endothermic or exothermic, on deep convection is examined. The effect on the flow is negligibly small in both cases.

Introduction

It is generally agreed that polymorphic phase transformations are the cause of the seismic transition zone between 300 and 1000 km in the Earth's mantle. The first major discontinuity at 350–400 km depth is related to the (exothermic) olivine-spinel transition (Ringwood 1975). The main candidates for the other important discontinuity at $\cong$ 650 km are either decomposition of the spinel-phase to mixed oxides (e.g. Ming & Bassett 1975) or to perovskite and periclase (Ito 1977). However, the idea that the discontinuity is caused by a sudden change in chemical composition still has some support (Liu 1979). A chemical boundary would act as an obstacle to whole mantle convection.

Phase changes may affect mantle dynamics by several means: (a) Important physical properties can be expected to change across the boundary – especially the rheological behaviour of the material. Sammis *et al.* (1977) estimated the variations of viscosity by phase transitions to be less than one order of magnitude. Rheology may also be influenced by the effect of superplasticity connected with phase changes (Sammis 1976). These two effects are ignored in the present investigation. (b) The release or absorption of latent heat

*Former name: U. Kopitzke. Now at Max-Planck-Institut für Chemie, Saarstrasse 23, D-6500 Mainz, West Germany.

from material undergoing the transition influences the temperature field, and via thermal expansion the driving buoyancy forces as well. (c) Lateral temperature differences connected with convection cause a distortion of the phase boundary's depth. Such distortion is accompanied by significant buoyancy forces.

Since the beginning of plate tectonics and mantle convection theory, there have been controversial opinions about the precise influence of phase boundaries on mantle dynamics. Knopoff (1964) argued that the transition would prevent convection currents from crossing the boundary. Ringwood (1975, pp. 517 ff.) thought, that at least the rising column of a convection cell – driven by a small superadiabatic gradient – faces difficulties in traversing the transition zone. In this zone – which may be some tens of kilometres wide – the adiabatic gradient is about one order of magnitude steeper than outside. This enlarged gradient seemed to be hard to overcome. However, by linear stability analysis it was proved that these assumptions are wrong. The method of linear stability analysis was applied by various authors to convection with both univariant or divariant phase changes (Schubert & Turcotte 1971; Busse & Schubert 1971; Schubert, Yuen & Turcotte 1975); they found out that phase boundaries may promote or hinder convection, depending on the actual choice of parameters, but they would hardly act as a principal barrier.

The linear stability analysis is only valid for infinitesimal slow convection; however, mantle convection is believed to be very vigorous. Thus finite amplitude considerations are necessary. The influence of phase changes in the descending slab – where much of the driving buoyancy force seems to be concentrated – is investigated by Schubert & Turcotte (1971) and Schubert *et al.* (1975). Concerning the exothermic olivine-spinel transition, they show that the effect of phase boundary elevation – which enhances the negative buoyancy of the slab – prevails over the counteracting effect of latent heat release. Thus olivine-spinel transition promotes slab subduction. The body force due to phase boundary distortion is smaller, but just in the same order of magnitude as the force due to normal thermal contraction.

Regarding a possibly endothermic spinel–post-spinel transition, things are the other way round. Nevertheless, it is unlikely that an endothermic boundary would restrain the slab from penetrating the deep mantle.

So far, the only finite amplitude model of a complete convection cell containing a phase boundary has been developed by Richter (1973). He found that a boundary with properties like the olivine-spinel transition doubles the amplitude of convection (flow velocity etc.) at Rayleigh numbers above 1000, leaving the stream pattern nearly unchanged. However, these results are deduced from a simple Rayleigh–Bénard model with low supercritical values of the Rayleigh number. To extrapolate them to the mantle seems questionable, because there the Rayleigh number is assumed to be between 10^2 and 10^5 times critical, and viscosity variations of several orders of magnitude may play an important role. Therefore it seems desirable to investigate the influence of phase transitions in a more realistic model of mantle convection.

In a previous paper (Kopitzke 1979, hereafter paper 1), I presented a dynamical finite element model of mantle convection which allows the choice of different penetration depths of the flow. A sub-oceanic convection cell is modelled and steady state is achieved. In contrast to previous dynamical models, it is possible to obtain plate-like behaviour of the upper thermal boundary layer (= lithosphere) by a special choice of viscosity distribution. In the present investigation phase boundaries are included in this model. Calculations of upper mantle convection with exothermic olivine-spinel boundary and of deep convection with olivine-spinel boundary alone and additionally with either exothermic or endothermic spinel–post-spinel transitions are carried out. The results are compared with equivalent models without phase changes.

Governing equations and numerical treatment of phase boundaries

The governing equations of two-dimensional convection in a variable viscosity fluid are discussed in paper 1 and elsewhere (e.g. Andrews 1972; Turcotte, Torrance & Hsui 1973). Infinite Prandtl number is assumed, the Boussinesq approximation is applied, and the effects of adiabatic gradient, frictional heating, inner heat sources and bottom heat flux, and the depth dependence of thermal diffusivity and thermal expansivity are taken into consideration. The equations are solved by a finite element method with bicubic and biquadratic spline functions on a rectangular grid. Ritz-Rayleigh variational method is applied to the hydrodynamic equation, and a special 'upwind' weighted residual method to the temperature equation. Both equations are solved iteratively until steady state is (approximately) reached. The numerical grid is the same as in paper 1, containing 32×11 and 32×16 elements respectively. It allows fine resolution in the lithosphere and at the lateral margins of the cell. The accuracy and reliability of this method was confirmed by a number of tests, where the finite element results were compared with the analytical solution (in cases of most simple problems), with own finite difference results (simple convection problems), and with the models of Turcotte *et al.* (1973) and De Bremaecker (1977) (sophisticated convection models). A further hint is the agreement of the total surface heat flow with the 'input heat' of the cell, which are equal within 1 per cent. I estimate the overall accuracy to be better than 10 per cent.

In order to calculate the buoyancy effect of phase boundary distortion, a phase function Γ and the dimensionless number R_p are introduced according to Richter (1973):

$$\Gamma = \begin{cases} 0 \text{ in the area of phase 1} \\ 1 \text{ in the area of phase 2} \end{cases}$$

$$R_p = \frac{g\,\Delta\rho\,h^3}{\kappa_0\,\eta_0}.$$

The hydrodynamic equation is then completed by a 'phase buoyancy term':

$$\left(\frac{\partial^2}{\partial z^2} - \frac{\partial^2}{\partial x^2}\right)\{\eta(\psi_{zz} - \psi_{xx})\} + 4\,\frac{\partial^2}{\partial x \partial z}(\eta\,\psi_{xz}) = Ra\,\frac{\alpha}{\alpha_0}\,\frac{\partial T}{\partial x} - R_p\,\frac{\partial \Gamma}{\partial x} \tag{1}$$

ψ: stream function, κ: thermal diffusivity,
η: viscosity, α: thermal expansivity,
g: gravity acceleration, $\Delta\rho$: density difference between the phases,
h: height of convection cell, ΔT: temperature difference between top and bottom,

$$Ra = \frac{\alpha_0 g\,\rho_0 \Delta T_0 h^3}{\kappa_0\,\eta_0}$$ Rayleigh number.

α_0, ΔT_0, κ_0, η_0, are properly defined mean or reference values of position dependent quantities.

The phase transitions are assumed to be univariant, therefore $\partial\Gamma/\partial x$ has the form of a δ-function. By application of the Ritz-Rayleigh method a matrix equation $A\,\mathbf{x} = \mathbf{r}$ is obtained. Its right side vector is to be completed by

$$r_i^{Ph} = -R_p \int \frac{\partial \Gamma}{\partial x}\,\psi_i\,dx\,dz \qquad i = 1 \ldots n, \tag{2}$$

ψ_i being a base spline function. In order to evaluate this integral numerically, the phase boundary is approached by a point chain (x_ν, z_ν) ($\nu = 1 \ldots \mathrm{NP}$; x is the horizontal coordinate). For each x_ν the appropriate depth z_ν is calculated from the actual temperature field

$$z_\nu = z_0 + \frac{\gamma}{\rho_0 g} \cdot T(x_\nu, z_\nu) \tag{3}$$

γ: Clapeyron slope of the phase transition.
Equation (2) can be approached by

$$r_i^{\mathrm{Ph}} = -R_\mathrm{p} \sum_{\nu=1}^{\mathrm{NP}} \psi_i(x_\nu, z_\nu) \cdot \frac{z_{\nu+1} - z_{\nu-1}}{2}, \tag{4}$$

so we have a simple formula to calculate the additional buoyancy effect of a phase boundary.

The specific latent heat of the phase change is calculated by the Clausius-Clapeyron equation

$$Q_\mathrm{L} = \gamma \cdot T_\mathrm{abs} \cdot \left(\frac{1}{\rho_2} - \frac{1}{\rho_1}\right) \simeq \gamma \cdot T_\mathrm{abs} \cdot \frac{\Delta\rho}{\rho^2}. \tag{5}$$

The heat actually released or absorbed per unit area and time at the boundary is proportional to the mass flux $\rho_0 \cdot v_\mathrm{s}$ through it (v_s being the velocity component perpendicular to the phase boundary).

$$Q_\mathrm{Ph} = \gamma \cdot T_\mathrm{abs} \cdot \frac{\Delta\rho}{\rho} \cdot v_\mathrm{s}. \tag{6}$$

The temperature effect of the phase transition is represented by point sources or sinks of heat in the model (at the phase points x_ν, z_ν). To calculate the total heat exchange between two points $x_{\nu-1}$, $x_{\nu+1}$ in the chain, v_s has to be integrated along a path between these points. The result is simply $\psi(x_{\nu+1}, z_{\nu+1}) - \psi(x_{\nu-1}, z_{\nu-1})$. Therefore the point source at x_ν, z_ν has the intensity

$$Q_\mathrm{Ph}^\nu = \frac{1}{2} \cdot \gamma \cdot \frac{\Delta\rho}{\rho} \cdot T_\mathrm{abs}(x_\nu, z_\nu) \cdot [\psi(x_{\nu+1}, z_{\nu+1}) - \psi(x_{\nu-1}, z_{\nu-1})]. \tag{7}$$

The supplement to the right side vector in the 'upwind' finite element formulation of temperature equation is obtained by multiplication of equation (7) with the values of the different weighting functions at the point under consideration (see also paper 1).

Structure of the model and choice of parameters

The model supposes sub-oceanic convection (no dynamically or thermally significant crust), the convection cell is assumed to be part of a periodic system of equal cells (symmetric lateral boundary conditions). The depth in the upper mantle model is confined to $\simeq$ 650 km, presuming either a sudden change of chemical composition or a strong increase of viscosity connected with the 650 km discontinuity, which could prevent convection from penetrating greater depth. The hydrodynamic boundary condition at the bottom is 'no slip'. In the deep convection model the depth is 1750 km – 60 per cent of real mantle depth – with free slip at the bottom. By the choice of this value, the volume of the plane model cell is made equal to the volume of a spherical mantle sector with the same surface area and 2900 km depth extent. Of course, concerning deep or whole mantle convection, it would be desirable to

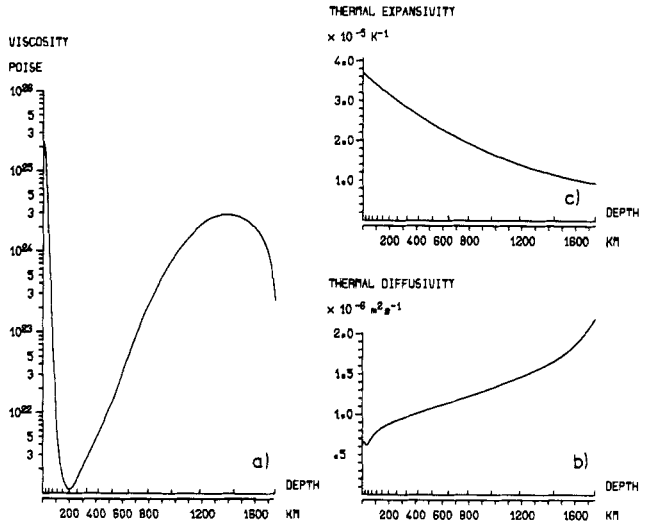

Figure 1. Depth profiles of important parameters applied in the model calculations. (a) Viscosity. (b) Thermal conductivity. (c) Thermal expansivity. When cutting off the parts below 643 km, the profiles appropriate to shallow models are obtained.

carry out really spherical model calculations. Then, however, one encounters considerable difficulties. The flat model may be useful as a first approach to the deep convection problem.

Rheology is assumed to be Newtonian and position-dependent (essentially depth-dependent). The depth-dependence of viscosity and other important parameters is shown in Fig. 1. The profile in Fig. 1(a) is only valid in the middle part of the cell. At the active margins of the lithosphere 'weak zones' of reduced effective viscosity are introduced. This reduction is arbitrary, but not implausible. At the spreading centre it is caused by hot material rising up to just some kilometres below the surface. In the bending region of lithospheric subduction it can be explained by 'non-linear weakening' due to increased stress level (Sleep 1975, paper 1). These weak zones are necessary to make the surface boundary layer behave like a rigid plate, which means that the surface velocity is constant over the entire length, heat flux and topography show the expected dependence, etc. Although the applied rheology is simple, results are much better than in other dynamical models with sophisticated σ, p, T-controlled viscosity (e.g. De Bremaecker 1977). Compared with kinematic models with rigid plate (Parmentier & Turcotte 1978), the present one has the advantage to be fully dynamical, the driving mechanism is intrinsically included and the surface velocity need not be prescribed.

The total amount of heat input is determined in order to produce a mean surface heat flow of 67 mW m^{-2} (1.60 HFU). In the shallow model one-half of the heat comes from below, in the deep model one-third, the rest is generated by radioactivity inside the cell.

Concerning the olivine-spinel transition, $\Delta\rho/\rho$ is in the order of 8–10 per cent. Experimentally and theoretically derived values of γ are between 30 and 62 bar K^{-1} (Akimoto & Fusijawa 1968; Ringwood & Major 1970; Ito, Endo & Kawai 1971; Akimoto 1972). In the present model calculation $\Delta\rho/\rho \simeq 8$ per cent and $\gamma = 40$ bar K^{-1} are chosen. The spinel–post-spinel transition was formerly believed to be endothermic (Ahrens & Syono 1967; Bassett & Ming 1972; Ming & Bassett 1975), with $\gamma \simeq -13$ bar K^{-1}. However, Jackson, Liebermann & Ringwood (1974) argue that γ might be near zero or even distinctly positive. Therefore I carried out three different model calculations of deep convection with values of 0, −13, and +20 bar K^{-1} for the spinel–post-spinel transition. The first value means

virtually no effect of phase boundary flow and temperature field at all. $\Delta\rho/\rho$ of the spinel–post-spinel boundary is taken to be 8 per cent, the reference depth of transition (z_0 in equation 3) is chosen so that the olivine-spinel transition takes place in 350 km depth at 1400°C and the spinel–post-spinel transition in 650 km at 1500°.

Results

First the olivine-spinel transition is included into the models of shallow or deep convection (in the latter case with $\gamma(Sp–Psp) = 0$). The results are compared with those of 'phaseless' models. The mean value of viscosity η_0 is always adjusted in order to make the (mean) surface velocity 2.17 (±0.05) cm a^{-1} – a value that brings about an overturn time of the model plate equal to the mean overturn time in the Earth's plate system – 176 Myr (paper 1). Depending on the model, η_0 has to be reduced to 60–80 per cent of its standard value ($10^{22}P$), thus the profile in Fig. 1(a) has to be shifted slightly down. In Fig. 2 temperature distribution and stream function of the deep model are shown, and for a comparison stream pattern of the equivalent model without phase changes can be seen in Fig. 3. Apart from the olivine-spinel transition endothermic spinel–post-spinel transformation is also included in the model shown in Fig. 2. However, the latter phase change hardly contributes to the differences between Figs 2(a) and 3.

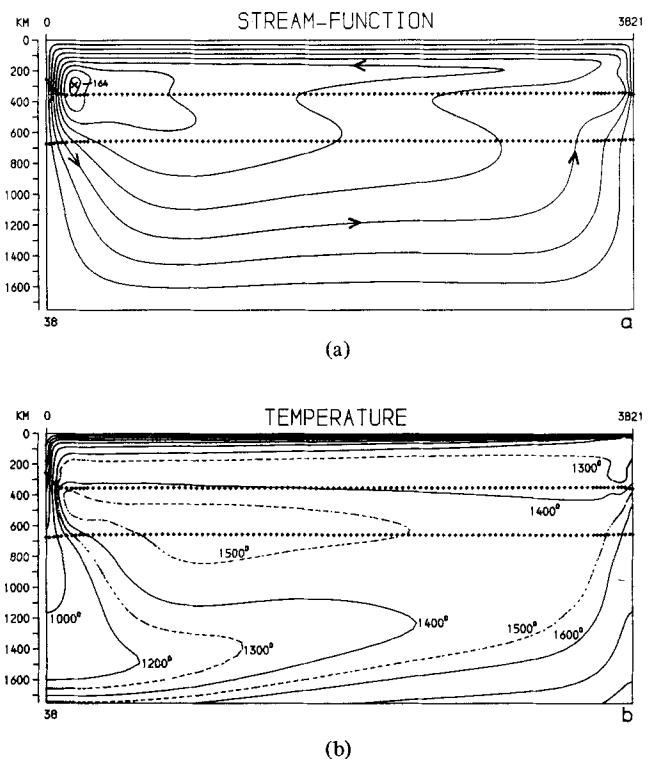

Figure 2. Deep convection model including exothermic olivine-spinel transition ($\gamma = 40$ bar K^{-1}) and endothermic spinel–post-spinel transition ($\gamma = -13$ bar K^{-1}). Phase boundaries are indicated by point chains. The Rayleigh number is 18.5×10^6. (a) Stream-function, contour interval is 20 (dimensionless) units, the maximum is indicated by an 'x'. (b) Isotherms, contour interval is 200°C, except for the broken lines.

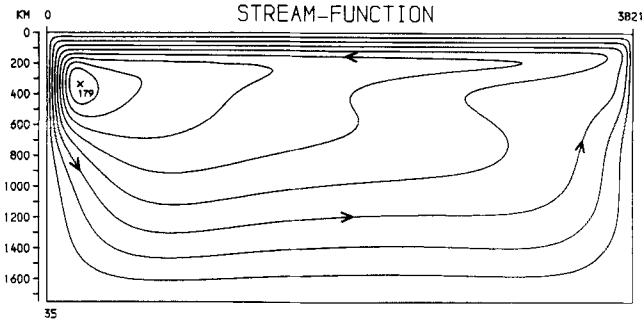

Figure 3. Stream pattern of deep convection model without phase changes. In order to obtain the same surface velocity as in the model shown before, the Rayleigh number must be 21×10^6, according to a 13 per cent decrease of viscosity.

The following differences are observed, when the exothermic olivine-spinel transition is taken into account:

(a) The viscosity must be enlarged by 13 per cent (deep convection) and 19 per cent (shallow convection) to obtain the same surface velocity. This means in turn, that the velocity will rise by 5–10 per cent if the viscosity is left unchanged, since at $Ra \gg Ra_{crit}$ velocity depends upon the Rayleigh number according to

$$v \simeq \sqrt{Ra} \simeq 1\sqrt{\eta}.$$

This enhancement is less than expected. Schubert & Turcotte (1971) calculated the negative buoyancy in the descending slab due to olivine-spinel boundary elevation to be 60 per cent of the buoyancy due to thermal contraction of the cold plate. Most of the additional energy input into the convection cycle by the phase boundary elevation in the descending slab seems to be released in the slab itself and in the region of lithospheric bending at the trench. Only a minor part is available to drive the plate more rapidly. This is in accordance with recent investigations about 'plate-driving forces' (e.g. Davies 1978), showing that the pull of the descending plate is counterbalanced by a strong 'trench-resistance'.

(b) The phase boundary is elevated by $\simeq 90$ km in the descending slab, according to horizontal temperature differences up to 900 K at 260 km depth. This is in agreement with thermal models of the slab (e.g. Toksöz, Minear & Julian 1971). Solomon & Paw U (1975) claimed to prove a similar elevation by seismic analysis. This contradicts Sung & Burns' (1976) idea that olivine might remain metastable in the cold descending slab and would not undergo the transition until a depth of 600 km. If the latter was right, it would cancel out most of the considerations about the influence of phase transitions on mantle dynamics.

Beneath the spreading-centre the olivine-spinel boundary is depressed about 30 km in the shallow model and just 5 km in the deep case, reflecting temperature differences of 300 and 50 K with respect to the normal mantle. This refutes Ringwood's (1975, pp. 517 ff.) thesis, that a rising column of hot material has to be $\simeq 200$ K warmer than the surrounding mantle in order to break through the phase transition zone.

(c) Only minor changes of stream pattern occur (compare Figs 2a and 3). Beneath the spreading centre the flow is compressed and accelerated by the phase boundary. Because of the high viscosity of the lithosphere, this effect is less pronounced in the descending slab. The phase transition slightly intensifies the tendency to reverse flow in the depth range 400–800 km (Fig. 2a) in the case of deep convection. Concerning shallow convection the differences in stream pattern are even less striking.

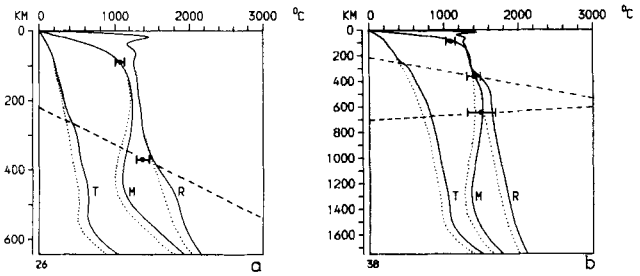

Figure 4. Geotherms. (a) Shallow convection. (b) Deep convection. The profiles are taken at the trench (T), in the middle of the cell (M), and under the ridge (R). The middle geotherm is representative for almost the entire length of the cell except the marginal regions. Solid lines belong to models including phase transitions, dotted lines to 'phase-less' convection. The position of olivine-spinel and (endothermic) spinel–post-spinel transition in the temperature–depth diagram are indicated by straight broken lines. Error bars at 90, 370 and 650 km depth indicate reference temperatures, contraint by several (indirect) observations (paper 1).

(d) In the deep model temperatures remain nearly unchanged above the olivine-spinel boundary. Below they are about 80–120 K higher in accordance with simple estimates, which predict a temperature rise

$$\Delta T = Q_L/c_p \simeq \gamma \cdot T_{abs} \cdot \Delta\rho/(\rho^2 \cdot c_p)$$

just in the same order. The additional increase is nearly step-like (Fig. 4). In the case of shallow convection, temperatures below 400 km are also about 100 K higher, but the increase is only step-like in the marginal regions (spreading/subduction zone). In the main part of the cell it is distributed over the depth range from 150–400 km (Fig. 4a). In contrast to the shallow model, there is significant mass flux through the phase boundary even outside the marginal regions, if convection is allowed to penetrate the lower mantle. Vertical velocity is in the order of 0.05 cm a^{-1}. Thus a certain amount of latent heat is released and removed by convection before it can spread out conductively. A step in the geotherm is the consequence.

(e) The surface topography of the cell was calculated by a method given by De Bremaecker (1976). However, the level of isostatic adjustment (where normal vertical stress $-p + \sigma_{zz}$ is assumed to be constant) is not placed at the bottom of the cell, like in De Bremaecker's model, but at the depth of minimum viscosity ($\simeq$ 200 km), which seems more reasonable. Lateral density differences below that level are compensated by undulations of the core–mantle boundary, which is assumed to be in 1750 km depth in both shallow and deep models. The surface topography displays all features that exist in the Earth's oceans (Fig. 5): a ridge with a central rift valley, rising up to 2500 m beneath sea-level, the ocean

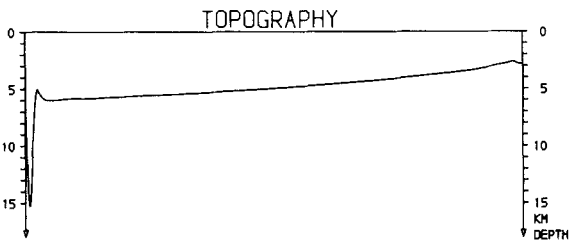

Figure 5. Surface topography (of deep convection model including both phase boundaries).

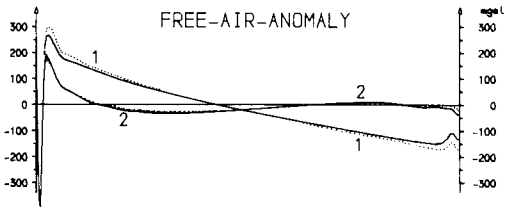

Figure 6. Free air gravity anomaly. The trench is on the left, the ridge on the right. (a) Shallow convection. (2) Deep convection. Dotted lines are from models without phase transitions.

basin with nearly 6000 m, the increase of depth follows roughly the $\sqrt{t}$ – law (Parsons & Sclater 1977). The trench with an outer ridge is displaced some 50 km from the edge of the cell, but is too deep (13–15 km). Only unimportant differences occur between shallow and deep models and between models with or without phase changes.

(f) Free air gravity anomaly was calculated by numerical integration, regarding the variation of surface topography, lateral density differences by thermal expansion inside the cell, phase boundary distortion, and the undulation of the core–mantle boundary. The small-scale variations are reflecting local topography, they are in part exaggerated (Fig. 6). Large-scale variations are unacceptably high in the shallow convection model (from over 100 mgal in the trench region to less than −100 mgal at the ridge), being even worse when the olivine-spinel transition is included. Concerning deep convection, they are more reasonable. The mean value in the trench region (the mean taken over ±1000 km) is 20–30 mgal, rather moderate despite the great small-scale variations. In the ridge region the mean value is nearly zero. This is in accordance with the observation that at trenches positive anomalies seem to prevail on a large scale, whereas no significant correlation of ridges to positive or negative gravity values could be found (e.g. Marsh & Marsh 1976). Concerning deep convection, differences are less pronounced, whether there is a phase change or not. The strong large-scale variations in shallow models seem to be caused by the lower thermal boundary layer of convection. In the deep model this layer has less influence due to different reasons, especially because its density differences are compensated by the isostatic undulation of the core–mantle boundary nearby.

(g) The stress distribution in the descending plate shows a change from tensile to compressive vertical stress between 320 and 340 km in each model. This depth of reversal is hardly influenced by the olivine-spinel transition, but the stress level is generally enlarged, especially in the vicinity of the phase boundary (stresses are generally in the order of 10 bar in the asthenosphere, 100 bar in the 'normal' lithosphere, and 0.4–1.3 kbar in the bending and subduction region of the lithosphere in the models). However, these results throw doubt on the assumption (e.g. Schubert *et al.* 1975), that the stress distribution generally observed in descending plates (tension in the upper, compression in the lower part) is a direct consequence of phase boundary distortion.

Inclusion of spinel–post-spinel transition

In two further model calculations, spinel–post-spinel transition with non-zero γ is included in the model with great depth extent. If the transition is exothermic ($\gamma = 20$ bar K^{-1}), its influence is similar to the olivine-spinel boundary, but more moderate according to a smaller value of γ and perhaps to the higher viscosity at the depth of transition. Plate velocity is increased by no more than 1 per cent (with η_0 unchanged). A temperature rise of $\simeq$ 50 K is connected with the phase boundary.

The influence of endothermic spinel–post-spinel transition ($\gamma = -13\,\text{bar}\,\text{K}^{-1}$) is almost negligible. The difference between Fig. 2(a) – where endothermic spinel–post-spinel transformation is also taken into account – and Fig. 3 are mostly caused by the olivine-spinel transition alone. The temperature is dropped by 30 K beneath the boundary. The plate velocity is lowered by 0.7 per cent. The relative amount of matter descending below the 650 km level (which is measured by comparing the maximum of stream function at 650 km and the absolute maximum) is unchanged (71 per cent), whether γ is negative or zero. Therefore the hindering action of the endothermic spinel–post-spinel boundary seems completely insignificant. The effect of 'mechanical brake' assumed by same authors (e.g. Kumazawa *et al.* 1974) does not exist. It seems unlikely that even a much lower γ could prevent convection currents from crossing an endothermic boundary (chemical heterogeneity of the mantle excluded).

Gravity and surface topography remain nearly unaffected by the spinel–post-spinel transition. Compressive stress between the two boundaries is slightly enlarged ($\simeq 10$ per cent) by an endothermic lower transition.

Conclusion

Although the finite element models contain a number of idealizations and uncertain assumptions, they can describe several important features quite well, for example the plate-like behaviour of the upper thermal boundary layer. Thus I expect the effects of phase transitions on real mantle convection not to be much different from those which turned out in these models. According to this, the effects of polymorphic phase transitions on mantle dynamics seem to have been mostly overestimated in the past. The additional driving action of olivine-spinel transition allows a viscosity increase of no more than 20 per cent to obtain the same plate velocity. The spinel–post-spinel transition – whether endothermic or exothermic – changes the plate velocity by 1 per cent or less. An endothermic phase change does not hinder the convection current to penetrate the lower mantle. The flow return is only slightly changed by phase boundaries. They have some influence on stress distribution and gravity anomalies, but this influence does not seem decisive. However, great differences appear in free air anomalies between shallow and deep convection models; the large-scale gravity variation is only acceptable in the latter case. Thus another argument in favour of whole mantle convection can be put forward.

The geotherm is altered by additional – often step like – temperature variations. Their magnitude can easily be calculated from the latent heat of the transition. It seems essential for the temperature variation to be step-like (that means a substantially increased gradient over no more than some tens of kilometres) that some mass flux actually crosses the boundary at the place under consideration. In the present investigation this is only valid in deep convection. (The gradient $\partial T/\partial p$ cannot be steeper than $1/\gamma$ (Gebrande private communication). That also implies that the transition zone is spread over at least some kilometres in a fast vertical flow, even in the univariant case.)

There are still many unknowns in the problem of mantle dynamics which can be expected to influence convection in a much more striking manner than the phase boundaries proved to do. Therefore it is surely admissible to neglect phase transitions in simple models of mantle dynamics.

Acknowledgment

This research is supported by 'Deutsche Forschungsgemeinschaft'.

References

Ahrens, T. J. & Syono, Y., 1967. Calculated mineral reactions in the earth's mantle, *J. geophys. Res.*, **72**, 4181–4188.

Akimoto, S., 1972. The system MgO-FeO-SiO_2 at high pressures and temperatures – phase equilibria and elastic properties, *Tectonophys.*, **13**, 161–187.

Akimoto, S. & Fusijawa, H., 1968. Olivine-spinel solid solution equilibria in the system Mg_2SiO_4–Fe_2SiO_4, *J. geophys. Res.*, **73**, 1467–1479.

Andrews, D. J., 1972. Numerical simulation of sea-floor spreading, *J. geophys. Res.*, **77**, 6470–6481.

Bassett, W. A. & Ming, L. C., 1972. Disproportionation of Fe_2SiO_4 to 2FeO + SiO_2 at pressures up to 250 kbar and temperatures up to 3000°C, *Phys. Earth planet. Int.*, **6**, 154–160.

Busse, F. & Schubert, G., 1971. Convection in a fluid with two phases, *J. Fluid Mech.*, **46**, 801–812.

Davies, G. F., 1978. The role of boundary friction, basal shear stress, and deep mantle convection in plate tectonics, *Geophys. Res. Lett.*, **5**, **161–164.**

De Bremaecker, J.-Cl., 1976. Relief and gravity anomalies over a convecting mantle, *Geophys. J. R. astr. Soc.*, **45**, 349–356.

De Bremaecker, J.-Cl., 1977. Convection in the earth's mantle, *Tectonophys.*, **41**, 195–208.

Ito, E., 1977. The absence of oxide mixture in high-pressure phases of Mg-silicates, *Geophys. Res. Lett.*, **4**, 72–74.

Ito, E., Endo, S. & Kawai, N., 1971. Olivine-spinel transformation in a natural forsterite, *Phys. Earth planet. Int.*, **4**, 425–428.

Jackson, I. N., Liebermann, R. C. & Ringwood, A. E., 1974. Disproportionation of spinels to mixed oxides: effects of inverse character and implications for the mantle, *Earth planet. Sci. Lett.*, **24**, 203–208.

Kopitzke, U., 1979. Finite element convection models: comparison of shallow and deep mantle convection, and temperatures in the mantle, *J. Geophys.*, **46**, 97–121.

Knopoff, L., 1964. The convection current hypothesis, *Rev. Geophys.*, **2**, 89–123.

Kumazawa, M., Sawamoto, H., Ohtani, E. & Masaki, K., 1974. Post-spinel phases of forsterite and evolution of the earth's mantle, *Nature*, **247**, 356–358.

Liu, L., 1979. On the 650 km – discontinuity, *Earth planet. Sci. Lett.*, **42**, 202–208.

Marsh, B. D. & Marsh, J. G., 1976. On global gravity anomalies and two-scale mantle convection, *J. geophys. Res.*, **81**, 5267–5280.

Ming, L. C. & Bassett, W. A., 1975. The post-spinel phases in the Mg_2SiO_4–Fe_2SiO_4 system, *Science*, **187**, 66–68.

Parmentier, E. M. & Turcotte, D. L., 1978. Two-dimensional flow beneath a rigid accreting lithosphere, *Phys. Earth planet. Int.*, **17**, 281–289.

Parsons, B. & Sclater, J. G., 1977. An analysis of the variation of ocean floor bathymetry and heat flow with age, *J. geophys. Res.*, **82**, 803–807.

Richter, F. M., 1973. Finite amplitude convection through a phase boundary, *Geophys. J. R. astr. Soc.*, **35**, 265–276.

Ringwood, A. E., 1975. *Composition and Petrology of the Earth's Mantle*, McGraw-Hill, New York.

Ringwood, A. E. & Major, A., 1970. The system Mg_2SiO_4–Fe_2SiO_4 at high pressures and temperatures, *Phy. Earth planet. Int.*, **3**, 89–108.

Sammis, C. G., 1976. The effect of polymorphic phase boundaries on vertical and horizontal motions in the earth's mantle, *Tectonophys.*, **35**, 169–182.

Sammis, C. G., Smith, J. C., Schubert, G. & Yuen, D. A., 1977. Viscosity-depth profile of the earth's mantle: effect of polymorphic phase transitions, *J. geophys. Res.*, **82**, 3747–3761.

Schubert, G. & Turcotte, D., 1971. Phase changes and mantle convection, *J. geophys. Res.*, **76**, 1424–1432.

Schubert, G., Yuen, D. A. & Turcotte, D. L., 1975. Role of phase transitions in a dynamic mantle, *Geophys. J. R. astr. Soc.*, **42**, 705–735.

Sleep, N. H., 1975. Stress and flow beneath island arcs, *Geophys. J. R. astr. Soc.*, **42**, 827–857.

Solomon, S. C. & Paw U, K. T., 1975. Elevation of the olivine spinel transition in subducted lithosphere: seismic evidence, *Phys. Earth planet. Int.*, **11**, 97–108.

Sung, C.-M. & Burns, R. G., 1976. Kinetics of high-pressure phase transformations: implications to the evolution of olivine→spinel transition in the downgoing lithosphere and its consequences on the dynamics of the mantle, *Tectonophys.*, **31**, 1–32.

Turcotte, D. L., Torrance, K. E. & Hsui, A. T., 1973. Convection in the earth's mantle in *Methods in Computational Physics*, **13**, 431–454.

Toksöz, M. N., Minear, J. W. & Julian, B. R., 1971. Temperature field and geophysical effect of downgoing slab, *J. geophys. Res.*, **76**, 1113–1138.